Archives of Hydro-Engineering and Environmental Mechanics
Vol. 53 (2006), No. 3, pp. 267–291

Hydraulic Transients Analysis in Pipe Networks by the Method of Characteristics (MOC)

Roman Wichowski

Gdańsk University of Technology, Faculty for Civil and Environmental Engineering, ul. Narutowicza 11/12, 80-952 Gdańsk, Poland, e-mail: rwich@pg.gda.pl

(Received May 19, 2006; revised August 25, 2006)

Abstract

The paper presents results of an experimental and theoretical study of the hydraulic transients in straight pipes and numerical simulations of unsteady flow in pipe networks. A mathematical model consists of a set of partial differential equations of hyperbolic type, which have been transformed by the method of characteristics into ordinary differential equations which are solved by the predictor-corrector method. Experimental tests have been performed, in order to examine the hydraulic transients phenomenon, in a single straight steel pipe. The experiments were carried out in the hydraulic laboratory of the Institute of Water Supply and Water Engineering, Environmental Engineering Faculty, Warsaw University of Technology.

The numerical results show that the presented one dimensional model for a single pipe correctly describes the phenomenon since there is a good agreement with experimental maximum and minimum oscillations. In the paper, selected exemplary equations in a difference form for the pipe networks are also presented. One calculation example is given relating to the complex water-pipe network consisting of 17 loops, 48 pipelines and 33 nodes, supplied by two independent sources. Water-hammer throughout the whole pipeline network was caused by closing the gate valve at mid-point of one selected pipe. The results of the numerical calculations are presented in graphic form with respect to the final cross-sections of pipes.

Key words: hydraulic transients, method of characteristics, single pipe, experimental measurements, pipe networks, numerical simulations

1. Introduction

Hydraulic transients phenomenon is defined as unsteady flow or water hammer, which is transmitted as a pressure or water-hammer wave in the pipeline system (Chaudhry 1979).

Water-hammer in pipe networks result from an abrupt change in the flow velocity, by sudden changes in demand, abrupt closing or opening of liquid flow in a pipeline by means of various kinds of valves as well as uncontrolled pump

starting or stopping. A water-hammer phenomenon is important in design, maintenance and operation of water distribution systems. It can cause high pressures and negative pressures, and the pipe can be damaged in the short term through over-pressures. Thus the pipeline should be designed either with a suitable diameter and wall thickness or with appropriate water hammer control devices to withstand the associated maximum positive pressures and/or the minimum negative pressures.

Although computer modelling tools for simulation of hydraulic transient flows have been widely used in simple pipeline systems, little is known about the behaviour of the transient flow in complex pipe network systems. This phenomenon could be analyzed by several numerical methods. One of them is the method of characteristics which could be used for very complex systems, e.g. distribution pipes in water supply systems and pipe networks. The main purpose of this paper is to put forward the method of analysis of transient flows in water supply networks.

This subject-matter has been dealt with by several scientific papers only, mainly in the USA and Canada, cf. by Streeter (1967), Karney and McInnis (1992), McInnis and Karney (1995), Samani and Khayatzadeh (2002). Particularly interesting is the McInnis and Karney (1995) paper, where computerized transient-flow models have been used in the analysis of water-hammer events in topologically simple pipeline systems, and the performance of these models is well documented.

The present paper analyzes the unsteady flow in a single straight steel pipe and in the complex pipe network. Results of calculations for a single pipe are verified with measurements performed on the experimental installation in a hydraulic laboratory.

2. Solution of Unsteady Flows by the Method of Characteristics (MOC)

The mathematical model of unsteady flows of compressible liquid in elastic pipe is expressed by the set of two partial differential equations of the first order of hyperbolic type, i.e. a momentum equation (1), stating the dynamical equilibrium of the liquid particles in the cross section of pipe, and the continuity equation (2) derived from the mass conservation of the elastic fluid particles during their flow through an elastic pipe. To solve these equations advantage of the method of characteristics is commonly taken. For further analysis let us take down the simplified equations describing the unsteady flow phenomenon, which have the following form, cf. Chaudhry (1979), Evangelisti (1969), Fox (1977), Streeter (1967, 1972):

$$\frac{\partial H}{\partial x} + \frac{1}{gA}\frac{\partial Q}{\partial t} + R_0|Q|^m \mathrm{sgn} Q = 0, \tag{1}$$

$$\frac{\partial H}{\partial t} + \frac{a^2}{gA}\frac{\partial Q}{\partial x} = 0, \tag{2}$$

where:

- a – pressure wave speed,
- A – cross-sectional area of pipe,
- g – acceleration of gravity,
- H – pressure head (piezometric head),
- Q – fluid discharge,
- R_0 – pipe resistance coefficient,
- t – time,
- x – abscissa along the center line of the pipe.

The paper presents a solution of the set of equations (1) and (2) by the method of characteristics. At first it is necessary to transform them into suitable ordinary differential equations, referred to as compatibility equations on appropriate characteristics:

– compatibility equation on C_+ characteristics:

$$dH + \frac{a}{gA}dQ + R_0|Q|^m \operatorname{sgn} Q dx = 0 \tag{3}$$

$$\text{if} \quad \frac{dx}{dt} = a, \tag{3a}$$

– compatibility equation on C_- characteristics:

$$dH - \frac{a}{gA}dQ + R_0|Q|^m \operatorname{sgn} Q dx = 0 \tag{4}$$

$$\text{if} \quad \frac{dx}{dt} = -a. \tag{4a}$$

For the numerical calculation an iterative procedure, known as predictor-corrector method has been applied (Evangelisti 1969, Streeter 1972, Wichowski 1999, 2002). Equations (3) and (4) will be substituted by approximated difference equations, where finite increments Δx and Δt of independent variables x and t are used.

2.1. Equations for the Internal Points of the Grid of Characteristics

In the predictor-corrector method the corrected values of pressure head $H(x,t)$, and the volume discharge of the liquid $Q(x,t)$, or velocity $v(x,t)$ are calculated on the basis of the mean resistance of an elementary pipeline section related to the discharge flow or velocity value of the proceeding and the following time steps. Making use of compatibility equations (3) and (4) we can write down the approximate difference equations for the internal points of the grid of characteristics (Fig. 1).

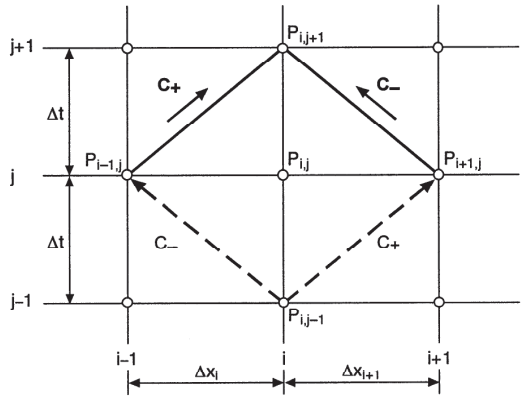

Fig. 1. Elementary mesh of characteristics grid for internal points

Predictor

C_+ compatibility equation:

$$H^p_{i,j+1} - H_{i-1,j} + Z_{i,j}\left(Q^p_{i,j+1} - Q_{i-1,j}\right) + R_{i,j}\left|Q_{i-1,j}\right|^m \operatorname{sgn} Q_{i-1,j} = 0. \tag{5}$$

C_- compatibility equation:

$$H^p_{i,j+1} - H_{i+1,j} - Z_{i+1,j}\left(Q^p_{i,j+1} - Q_{i+1,j}\right) - R_{i+1,j}\left|Q_{i+1,j}\right|^m \operatorname{sgn} Q_{i+1,j} = 0. \tag{6}$$

Corrector

C_+ compatibility equation:

$$\begin{aligned} &H_{i,j+1} - H_{i-1,j} + Z_{i,j}\left(Q_{i,j+1} - Q_{i-1,j}\right) + \\ &+0.5R_{i,j}\left(\left|Q_{i-1,j}\right|^m \operatorname{sgn} Q_{i-1,j} + \left|Q^p_{i,j+1}\right|^m \operatorname{sgn} Q^p_{i,j+1}\right) = 0. \end{aligned} \tag{7}$$

C_- compatibility equation:

$$\begin{aligned} &H_{i,j+1} - H_{i+1,j} - Z_{i+1,j}\left(Q_{i,j+1} - Q_{i+1,j}\right) + \\ &-0.5R_{i+1,j}\left(\left|Q_{i+1,j}\right|^m \operatorname{sgn} Q_{i+1,j} + \left|Q^p_{i,j+1}\right|^m \operatorname{sgn} Q^p_{i,j+1}\right) = 0. \end{aligned} \tag{8}$$

In the above equations i = subscript represents location along the x-axis, j = subscript represents time step, R is the hydraulic resistance of the pipe or its section while value Z is the so-called characteristic impedance of pipeline expressed by the formula:

$$Z = \frac{a}{gA}. \tag{9}$$

From the above equations we obtain the approximated value of flow $Q^p_{i,j+1}$ for the known conditions in the previous time step:

$$\begin{aligned} Q^p_{i,j+1} = \big[&\big(H_{i-1,j} - H_{i+1,j}\big) + \\ &- \big(R_{i,j}\,|Q_{i-1,j}|^m \operatorname{sgn} Q_{i-1,j} + R_{i+1,j}|Q_{i+1,j}|^m \operatorname{sgn} Q_{i+1,j}\big) + \\ &+ \big(Z_{i,j}\,Q_{i-1,j} + Z_{i+1,j}\,Q_{i+1,j}\big)\big] : \big(Z_{i,j} + Z_{i+1,j}\big). \end{aligned} \tag{10}$$

Having the approximated flow value at internal point $P_{i,j+1}$, it is now possible to find the corrected value of flow:

$$Q_{i,j+1} = Q^p_{i,j+1} + \Delta Q, \tag{11}$$

where: ΔQ is the value of the correction, derived on the basis of Eqs. (5)–(8).

2.2. Equations for the Boundary Points of the Grid of Characteristics

The boundary points of the system being influencing the interior points after the first time step Δt. Therefore, in order to complete the solution to any desired time, it is necessary to include the boundary conditions. At either end of a single pipe only one of the compatibility equations is available. For the left end (Fig. 2a) equation (4) along the C_- characteristics is valid, and for the right end (Fig. 2b) equation (3) along the C_+ characteristics is valid.

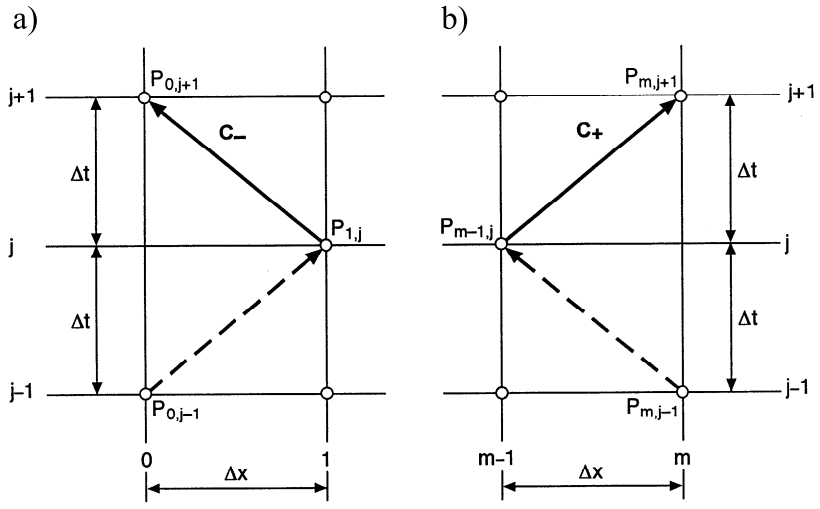

Fig. 2. Elementary meshes of grid of characteristics for boundary points: a) left end, b) right end

Left end (upstream end) (Fig. 2a):

Predictor
C$_-$ compatibility equation:

$$H^p_{0,j+1} - H_{1,j} - Z_{1,j}(Q^p_{0,j+1} - Q_{1,j}) - R_{1,j}\left|Q_{1,j}\right|^m \text{sgn } Q_{1,j} = 0, \tag{12}$$

where: $H^p_{0,j+1} = H(x,t)$ or $Q^p_{0,j+1} = Q(x,t)$.

Corrector
C$_-$ compatibility equation:

$$\begin{gathered} H_{0,j+1} - H_{1,j} - Z_{1,j}\left(Q_{0,j+1} - Q_{1,j}\right) + \\ -0.5R_{1,j}\left(\left|Q_{1,j}\right|^m \text{sgn } Q_{1,j} + \left|Q^p_{0,j+1}\right|^m \text{sgn } Q^p_{0,j+1}\right) = 0, \end{gathered} \tag{13}$$

where: $H_{0,j+1} = H(x,t)$ or $Q_{0,j+1} = Q(x,t)$.

Right end (downstream end) (Fig. 2b):

Predictor
C$_+$ compatibility equation:

$$H^p_{m,j+1} - H_{m-1,j} + Z_{m,j}\left(Q^p_{m,j+1} - Q_{m-1,j}\right) + R_{m,j}\left|Q_{m-1,j}\right|^m \text{sgn } Q_{m-1,j} = 0, \tag{14}$$

where: $H^p_{m,j+1} = H(x,t)$ or $Q^p_{m,j+1} = Q(x,t)$.

Corrector
C$_+$ compatibility equation:

$$\begin{gathered} H_{m,j+1} - H_{m-1,j} + Z_{m,j}\left(Q_{m,j+1} - Q_{m-1,j}\right) + \\ +0.5R_{m,j}\left(\left|Q_{m-1,j}\right|^m \text{sgn } Q_{m-1,j} + \left|Q^p_{m,j+1}\right|^m \text{sgn } Q^p_{m,j+1}\right) = 0, \end{gathered} \tag{15}$$

where: $H_{m,j+1} = H(x,t)$ or $Q_{m,j+1} = Q(x,t)$.

3. Experimental Measurements and Numerical Calculations of Unsteady Flows in Single Straight Pipes

3.1. Comparison of Numerical Calculations with own Experimental Results

For the purpose of obtaining empirical data, some experiments have been carried out on an installation consisting of a single straight steel pipe, situated at

the Hydraulic Laboratory of the Institute of Water Supply and Water Engineering, Environmental Engineering Faculty, Warsaw University of Technology. The experimental setup (Fig. 3) for investigating of unsteady flows is composed of a straight pipe (1), pressure tank (2) supplied with water from water supply system (10). A pressure reducing valve (3) designed to maintain a constant pressure in the tank (2) during the unsteady flow experiments was installed in the pipe supplying the tank with water.

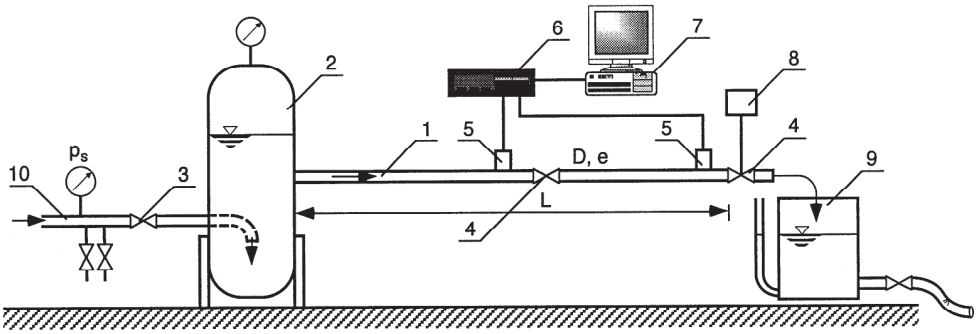

Fig. 3. Scheme of experimental installation: 1 – straight steel pipeline of $D_{in} = 42$ mm, 2 – pressurized tank, 3 – pressure reducing valve, 4 – ball valve, 5 – pressure transducers, 6 – extensometer amplifier, 7 – a computer with AD/DA card, 8 – digital time measurer, 9 – calibration tank, 10 – the pipe fed from the local water supply system (Wichowski 2002)

The tank (2) was connected with a straight steel pipe (1) of internal diameter $D_{in} = 42$ mm and total length $L = 41$ m. At the end of the pipeline a ball valve (4) closed manually was mounted. The closing time of the valve was measured by a digital time recorder (8) with accuracy of a thousandth of a second.

The pressure measuring system consisted of two strain gauges (5) with measuring ranges up to 1.2 MPa. One of the gauges was installed at the end of the pipeline before the ball valve, the other at its mid-length. The electric signal from the gauges was transmitted by a special screened cable to the extensometer bridge (6) where the signal was amplified and next conveyed to the computer with AD/DA 20 MHz card. The pressure was recorded at time intervals Δt of the order of 10^{-5} s. The pressure gauges had linear performance characteristics in the whole range of the measured pressure with a correlation coefficient $R = 0.999$.

The unsteady flows occurred when the ball valve (4) installed at the end of the pipeline was being closed. Prior to each closing procedure the steady-state flow measurement was taken using for this purpose an open tank (9) equipped with water gauge glass. The tank was located at the outlet of the pipe (1). The pressure heads $H(t)$ were recorded during the process of unsteady flow for different velocities w_0 of steady state (ranging from 0.136 to 0.463 m/s) which were measured by the volumetric method.

More than ten series of tests for a straight steel pipeline of constant internal diameter of 42 mm have been carried out. Each series was characterized by its own rate of flow in steady state, the pressure head in the tank and the closing time of the ball valve at the end of the pipeline.

In the experimental tests the following data were taken into consideration:

- steel pipeline of length $L = 41.0$ m,
- internal diameter of pipe $D_{in} = 42.0$ mm,
- thickness of pipe wall $e = 3$ mm,
- modulus of elasticity of pipe material $E_{st} = 2.06 \times 10^{11}$ Pa,
- bulk modulus of water $E_c = 2.19 \times 10^9$ Pa,
- water temperature $t_w = +4.5°\text{C}$,
- times of valve closure T_c different in each series of measurements.

The results of the measurements and calculations for the cross-section at the end of the straight pipe are presented in Figs. 4–6. The data relating to specific cases have been given in captions for the Figures.

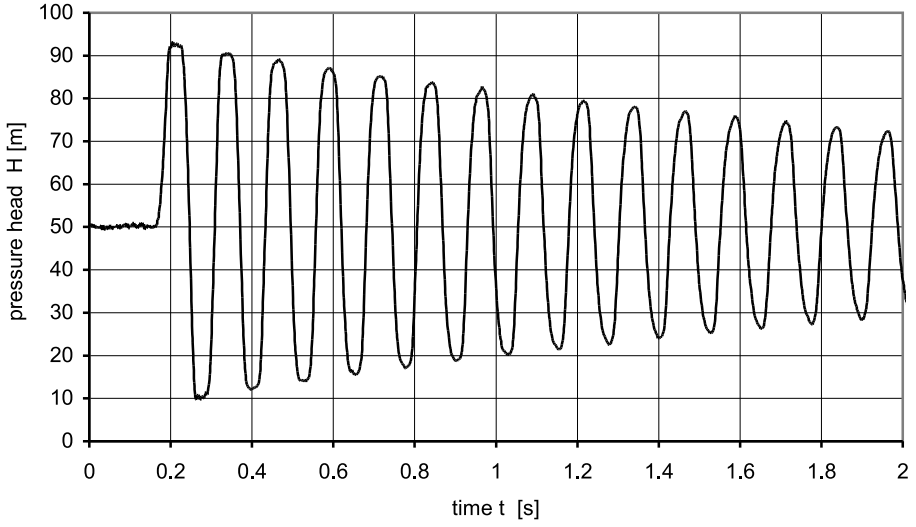

Fig. 4. Experimental pressure head oscillations at the end of straight steel pipeline: $L = 41$ m, $D_{in} = 42$ mm: $a = 1260$ m/s, $H_0 = 50.0$ m, $Q_0 = 0.453$ dm^3/s, $T_c = 0.034$ s

The numerical calculation results were obtained for the Courant number $C_r = 1.00$, calculated for a pipe of $L = 41$ m divided into 30 sections with pressure velocity $a = 1260$ m/s based on measurements and the time step $\Delta t = 0.0011$ s.

$$C_r = \frac{a \cdot \Delta t}{\Delta x} = \frac{1260 \cdot 0.001085}{1.367} = 1.00.$$

As can be seen from the comparison of the diagrams presented in Figs. 4 and 5 the compatibility of the extreme pressure head values for the valve cross section appears to be quite satisfactory. The computational value of the friction factor λ was 0.055. The maximum pressure head value calculated for the valve section is smaller than the measured one by 1.13 m which is barely 1.2%. In the discussion of the results the minimal pressure values were not taken into account since in calculations of strength these values are ignored because they have no significant influence on the pipe's strength or the choice of safety devices. In some cases excessively low pressures can lead to the release of large amounts of dissolved air, and extensive vaporization of the liquid can occur if the pressure drops to the liquid vapor pressure.

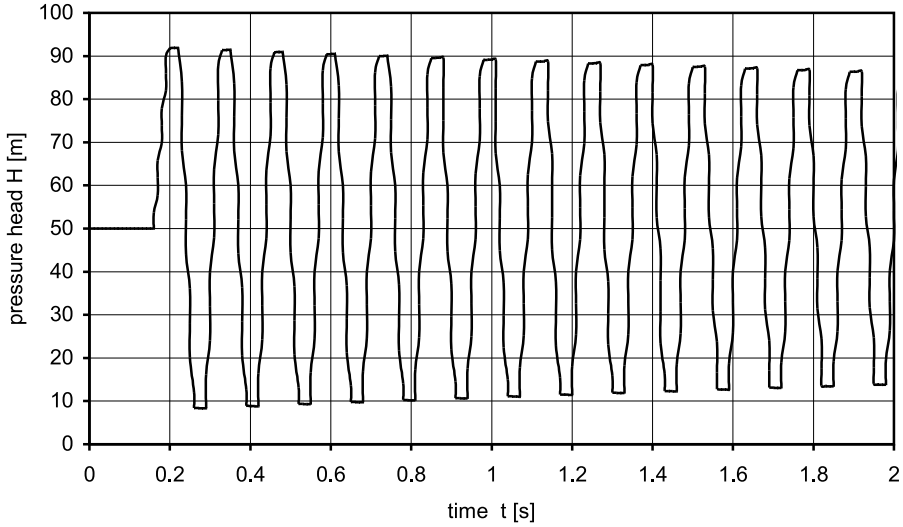

Fig. 5. Numerical calculation of pressure head oscillations at the end of straight steel pipeline: $L = 41$ m, $D_{in} = 42$ mm, $a = 1260$ m/s, $H_0 = 50.0$ m, $Q_0 = 0.453$ dm^3/s, $T_c = 0.034$ s, $\lambda = 0.055$

In Table 1 the extreme values of pressure heads obtained from measurements and calculations are presented (Wichowski 2002).

Table 1. Extreme values of pressure heads $H(t)$ from measurements and numerical calculations

$H_0 = 50.0$ m, $Q_0 = 0.453$ dm^3/s, $T_c = 0.034$ s, $a = 1260$ m/s								
measured extreme pressure [m]				calculated extreme pressure [m]				
ball valve		mid-length of pipe		λ	ball valve		mid-length of pipe	
H_{max}	H_{min}	H_{max}	H_{min}		H_{max}	H_{min}	H_{max}	H_{min}
93.07	9.80	92.19	11.35	0.055	91.94	8.50	90.80	10.20
				0.250	91.73	9.40	88.90	13.23

The analysis of the calculation and measurement results also reveals some discrepancies dealing with the total attenuation time of the pressure oscillation

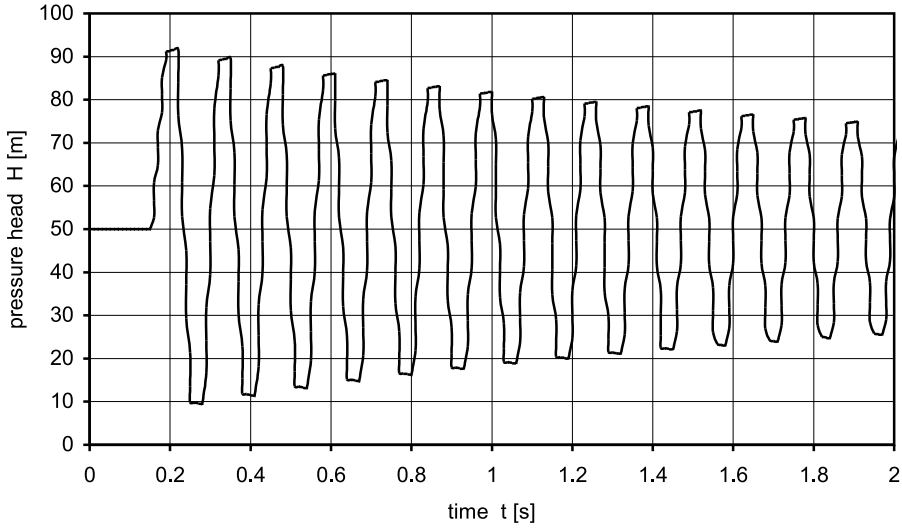

Fig. 6. Numerical calculation of pressure head oscillations at the end of straight steel pipeline: $L = 41$ m, $D_{in} = 42$ mm, $a = 1260$ m/s, $H_0 = 50.0$ m, $Q_0 = 0.453$ dm^3/s, $T_c = 0.034$ s, $\lambda = 0.250$

and the compatibility of its phases. The real attenuation times relating to all cases under test were much shorter than the times resulting from calculations, which in general took about 10 seconds in the experiments. The only physical parameter of the mathematical model having a qualitative effect on the calculation result is the friction factor λ. Analyzing some professional literature on this subject (Axworthy et al 2000, Bergant and Simpson 1994, Bergant et al 1999, Pezzinga and Scandura 1995) it is possible to conclude that the attenuation of pressure oscillation is resulting because of the viscous forces of fluid, and the value of τ_e denoting the tangential stresses on the pipe surface is expressed by the classical hydraulic relations, that is the Darcy-Weisbach equation.

In order to improve extreme pressures compatibility, modification has been made of the friction element by assuming much greater values of the linear friction factor λ as compared with the ones used in the steady state analysis. In our case the value of friction factor λ was 0.055, while the value adopted to improve the compatibility of the calculation and measurement of pressure head results amounted to 0.25 which is about 4.5 times greater. The calculation results for the corrected value of friction factor λ are presented in Fig. 6.

Results of measurements and calculations obtained by various authors (e.g. Axworthy et al 2000, Bergant et al 1999, Brunone et al 1991, Pezzinga and Scandura 1995, Vitkovsky et al 2000) prove that the traditional models of unsteady flow analyses make it possible to calculate the extreme values at the outset of the phenomenon, with great accuracy. However, the discrepancy between the calculations and the measurement results is not satisfactory regarding the further stages of both the extreme values and the compatibility relating to the calculated and

measured pressure phases. The calculations provide the higher pressure heads in all phases except the first.

3.2. Comparison of Numerical Calculations with the Measurements Made by G. Pezzinga

In the paper advantage is also taken of the experimental measurements of transients flow carried out by G. Pezzinga on the experimental installation at the hydraulic laboratory of the Institute of Hydraulics, Hydrology and Water Management, University of Catania (Italy). A description of the experiments can be found in the paper by Pezzinga and Scandura (1995), Pezzinga (2000) and in the paper by Axworthy et al (2000). The author obtained some original results for 3 series of experimental investigations carried out by G. Pezzinga who granted permission to make use of the results in the paper.

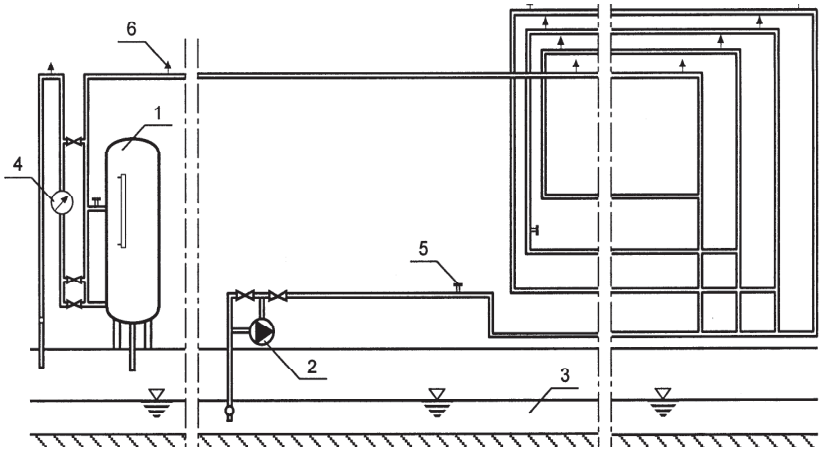

Fig. 7. Experimental installation made by G. Pezzinga (1995, 1999, 2000, Axworthy et al 2000): 1 – pressure tank, 2 – centrifugal pump, 3 – open channel, 4 – electromagnetic flow meter, 5 – strain gauge pressure transducer, 6 – air release

A zinc-plated steel of length $L = 143.7$ m and nominal diameter DN50 (internal diameter 53.2 mm, wall thickness 3.35 mm, modulus of elasticity $E = 2.06 \times 10^{11}$ Pa, absolute roughness 0.11 mm) was supplied with water by a centrifugal pump mounted at one of the ends. The opposite end of the pipe was connected with a pressure tank of 1.0 m^3 total capacity. Measurements of total discharge were made by an electromagnetic flow-meter. The line pressure was measured by strain gauge pressure transducers which have a range of $0 \div 10$ bar and a maximum error of $\pm 0.5\%$ of full-scale pressure. The signal from the pressure transducers was sampled with a frequency of 200 Hz and registered with high accuracy system with 16-bit card computer and specialist software used to transform and register the measurement results. Along the conduit were installed air

relief valves and cut-off ball valves aimed at closing various segments of the conduit and enabling tests on pipes of different length (Fig. 7) (Pezzinga, Scandura 1995, Pezzinga 1999, Pezzinga 2000).

Each experimental run commenced from steady-state conditions followed by manual closing of a ball-valve at the upstream end of the main pipe, isolating the pump during the transients conditions. The valve closure was estimated to take about 0.04 seconds. Simultaneously, the discharge downstream of the pressure tank was intercepted by a ball-valve.

The experimental tests included two series of measurements for the total length of conduit of $L_1 = 143.7$ m and two series of measurements for a pipe of length $L_2 = 72.8$ m. The mean temperature of water supplying the pipeline was $+15^{\circ}$C, the kinematic viscocity coefficient was $\nu = 1.14 \times 10^{-6}$ m^2/s, whereas the bulk modulus of water elasticity was $E_w = 2.14 \times 10^9$ Pa. In the paper results for the first series of measurements in the cross-section at the end of pipe (Figs. 8, 9 and 10) and for the cross-section at mid-length of pipe (Figs. 11, 12 and 13) are presented.

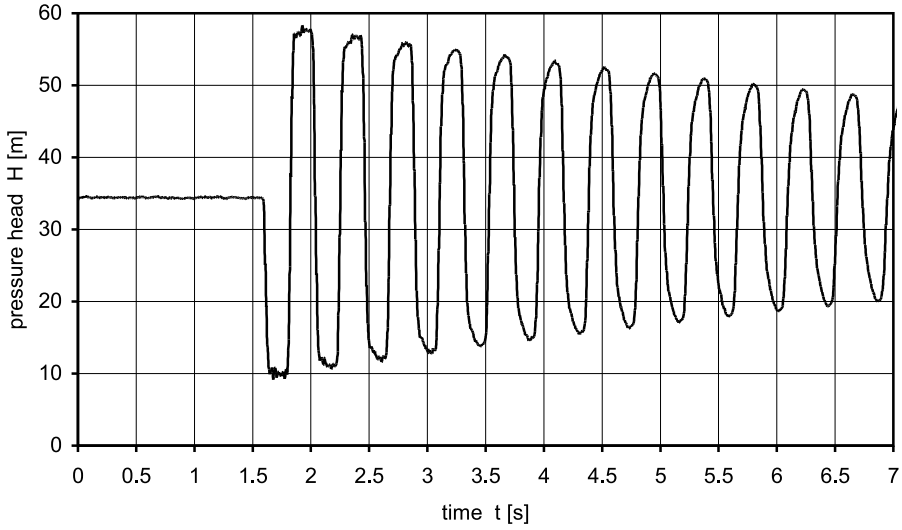

Fig. 8. Experimental pressure head oscillations during measurements made by Pezzinga (Pezzinga, Scandura 1995, Pezzinga 1999, Pezzinga 2000) at the end of straight steel pipeline: $L = 143.7$ m, $D_{in} = 53.2$ mm, $H_0 = 34.5$ m, $Q_0 = 0.4$ dm^3/s, $T_c = 0.04$ s

In the measurements made by G. Pezzinga the following data were taken into consideration (Pezzinga and Scandura 1995, Pezzinga 1999, Pezzinga 2000):

- length of steel pipeline $L = 143.7$ m,
- internal diameter of pipe $D_{in} = 53.2$ mm,
- thickness of pipe wall $e = 3.35$ mm,

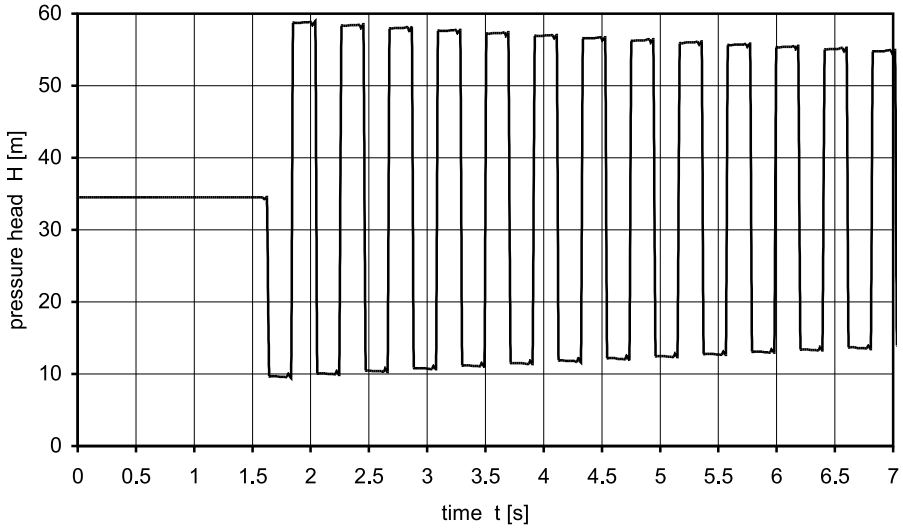

Fig. 9. Numerical calculation of pressure head oscillations at the end of straight steel pipeline: $L = 143.7$ m, $D_{in} = 53.2$ mm, $H_0 = 34.5$ m, $Q_0 = 0.4$ dm^3/s, $T_c = 0.04$ s, $\lambda = 0.035$

- absolute roughness $k = 0.01$ mm,
- modulus of elasticity of pipe material $E_{st} = 2.06 \times 10^{11}$ Pa,
- bulk modulus of water $E_c = 2.14 \times 10^9$ Pa,
- water temperature $t_w = +15^\circ$C,
- times of valve closure $T_c = 0.04$ s,
- volume of the pressure tank $V = 1.0$ m^3.

The extreme values of measurements made by Pezzinga and calculations made by the author are given in Table 2 (Pezzinga, Scandura 1995, Pezzinga 1999, Pezzinga 2000).

As can be concluded from comparison of the diagrams with the measurements made by Pezzinga (Fig. 8) and calculations made by the author (Fig. 9 and Fig. 10), the compatibility of the extreme values is quite good as the maximum pressure head calculated for the cross-section at the ball-valve is greater by 0.48 m than the measured value, which is less than 1%, whereas the minimum calculation value is bigger by 0.23 m than the measured value, which is about 3.5%.

In the final stage, the calculated value for the coefficient of linear friction resistance λ is encumbered with much greater differences between the calculation and measurement results. With regard to the cross-section at the ball-valve the maximum calculated pressure is greater by 6.13 m as compared with the measured one, which is 12.6%. The calculated minimum pressure head value for the cross-section at the ball-valve is lower than the measured magnitude by 6.50 m, which is 32.5% (see Table 2), whereas the calculated minimum pressure value at

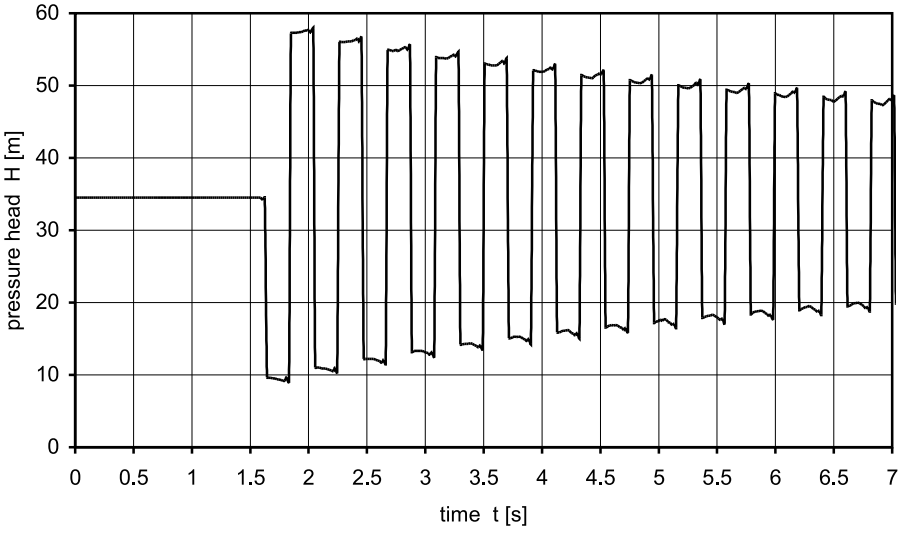

Fig. 10. Numerical calculation of pressure head oscillations at the end of straight steel pipeline: $L = 143.7$ m, $D_{in} = 53.2$ mm, $H_0 = 34.5$ m, $Q_0 = 0.4$ dm^3/s, $T_c = 0.04$ s, $\lambda = 0.150$

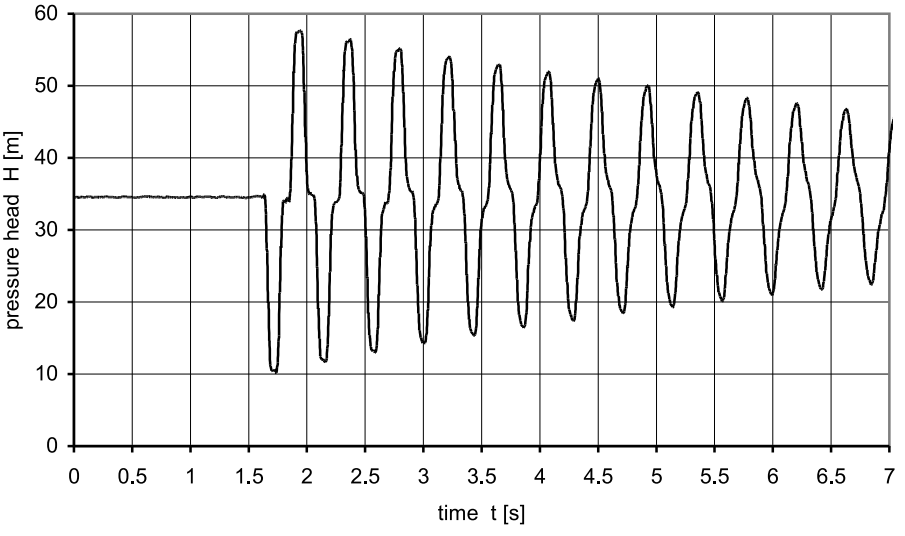

Fig. 11. Experimental pressure head oscillations during measurements made by Pezzinga (1995, 1999, 2000) at mid-length of straight steel pipeline: $L = 143.7$ m, $D_{in} = 53.2$ mm, $H_0 = 34.5$ m, $Q_0 = 0.4$ dm^3/s, $T_c = 0.04$ s

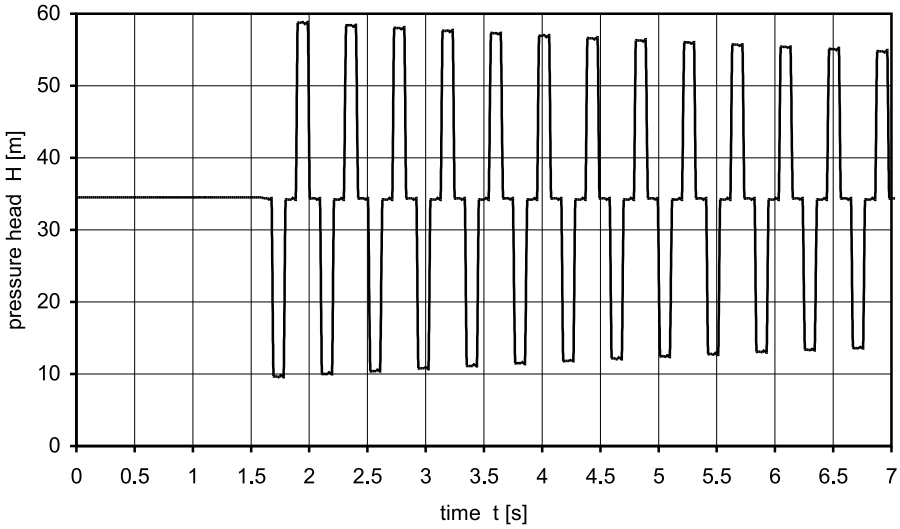

Fig. 12. Numerical calculation of pressure head oscillations at mid-length of straight steel pipeline: $L = 143.7$ m, $D_{in} = 53.2$ mm, $H_0 = 34.5$ m, $Q_0 = 0.4$ dm^3/s, $T_c = 0.04$ s, $\lambda = 0.035$

mid-length of the pipe is smaller than measured data by approximately 8.84 m being about 39.4% (see Table 2).

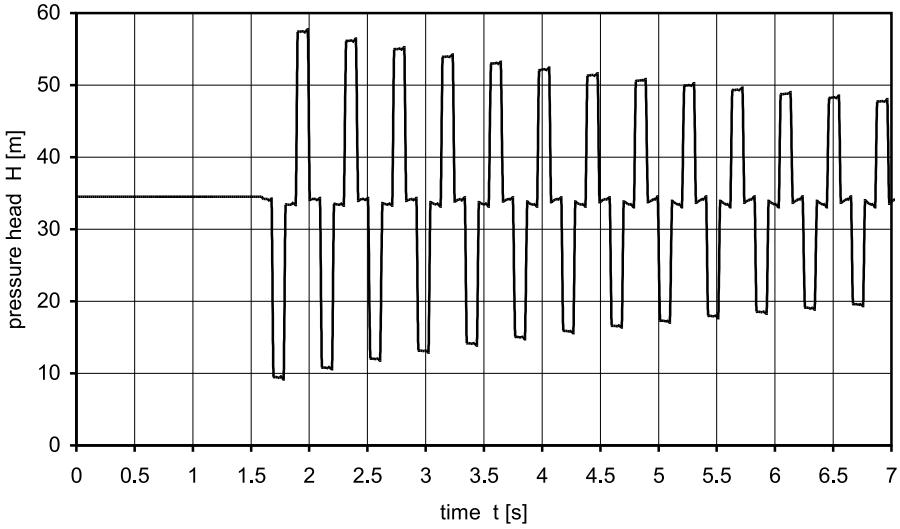

Fig. 13. Numerical calculation of pressure head oscillations at mid-length of straight steel pipeline: $L = 143.7$ m, $D_{in} = 53.2$ mm, $H_0 = 34.5$ m, $Q_0 = 0.4$ dm^3/s, $T_c = 0.04$ s, $\lambda = 0.150$

As follows from the diagrams presented on Figs. 8 to 13 and Table 2 the measurement results indicate significantly larger pressure attenuation compared

Table 2. Extreme values of pressure heads $H(t)$ from measurements made by Pezzinga and numerical calculations by the author: $L = 143.7$ m, $D_{in} = 53.2$ mm, $H_0 = 34.5$ m, $Q_0 = 0.4$ dm^3/s, $T_c = 0.04$ s

Initial phase of transients								
extreme measured pressure heads [m]				extreme calculated pressure heads [m]				
ball-valve		mid-length		λ	ball-valve		mid-length	
H_{max}	H_{min}	H_{max}	H_{min}		H_{max}	H_{min}	H_{max}	H_{min}
58.32	9.18	57.64	10.38	0.035	58.80	9.50	58.80	9.60
				0.150	57.90	9.00	57.70	9.20
Final phase of transients								
48.77	20.00	46.80	22.44	0.035	54.90	13.50	54.90	13.60
				0.150	48.60	18.80	48.00	19.40

with the calculated values obtained as a consequence of making use in the calculation of friction in unsteady-state. Under real conditions the pressure head attenuation is greater in every case, which was proved by the experiments carried out by Pezzinga (Pezzinga and Scandura 1995), and the experimental investigation performed by the author on a model in the hydraulic laboratory discussed in the previous chapter.

To improve the compatibility of the calculation and measurements results, procedures to follow further calculations were made for the same hydraulic system on the assumption that friction factor $\lambda = 0.15$, i.e. more than four times greater than the value used in calculation in steady-state condition. The calculation results of pressure head oscillations for higher friction factor values are presented in Fig. 10 for cross section at the ball-valve and in Fig. 13 for the cross-section at mid-length of pipe.

As it is possible to note from the comparison of the diagrams presented in Figs. 8 to 13, the compatibility of calculation and measurements obtained for the extreme values both in the initial phase of the unsteady flow and in the final one is quite good and results of such calculation could be used for evaluation of pipe strength and for selection of safety devices used in water supply systems.

4. Analysis of Unsteady Flows in Water-Pipe Networks

In the water supply systems, as well as in district heating networks and industrial complex pipelines systems branching pipes are generally used, i.e. forking and connecting pipes. Systems of this kind occur in both distributed and looped pipe networks, which consist of single transit pipelines, water mains, and distributing pipes. The junction points or nodes in systems of branching pipes are dealt with like appropriate internal boundary points. Thus, each junction point or node W (Fig. 14) is right end boundary with respect to an elementary section or sections of pipelines on its, or their, left side and simultaneously a left end boundary for an elementary section or sections of pipelines on the right side of that point.

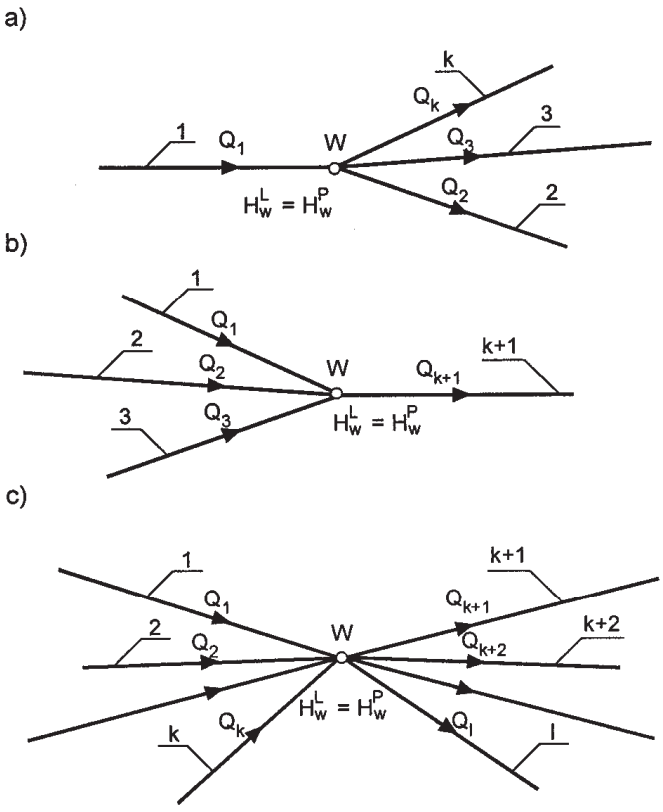

Fig. 14. Examples of pipelines with different nodes: a) node with forking pipelines, b) node with connecting pipes, c) complex node

In all cases the continuity equation, i.e. equilibrium condition of the sums of inflows to the junction and the sums of outflows from the junction, is utilized as the boundary condition:

$$\sum Q_{\text{inflows}} = \sum Q_{\text{outflows}}. \tag{16}$$

It is additionally assumed that the pressure heads in the neighbourhood of point W are equal:

$$H_w^l = H_w^r. \tag{17}$$

Supplementary equations are the compatibility equations with respect to appropriate characteristics depending on the case under consideration. Adequate equations for commonly applied branching junctions in complex pipeline systems will be presented below. For the junctions of forking pipelines (Fig. 14a) the following compatibility equations can be written:

$$
\begin{gathered}
H^{(1)}_{m1,j+1} - H^{(1)}_{m1-1,j} + Z^{(1)}_{m1,j}\left(Q^{(1)}_{m1,j+1} - Q^{(1)}_{m1-1,j}\right) + \\
+R^{(1)}_{m1,j}\left|Q^{(1)}_{m1-1,j}\right|^{m}\operatorname{sgn} Q^{(1)}_{m1-1,j} = 0 \\
H^{(2)}_{0,j+1} - H^{(2)}_{1,j} - Z^{(2)}_{1,j}\left(Q^{(2)}_{0,j+1} - Q^{(2)}_{1,j}\right) - R^{(2)}_{1,j}\left|Q^{(2)}_{1,j}\right|^{m}\operatorname{sgn} Q^{(2)}_{1,j} = 0 \\
\cdots\cdots\cdots\cdots\cdots\cdots\cdots\cdots\cdots\cdots\cdots\cdots\cdots\cdots\cdots\cdots\cdots\cdots\cdots\cdots\cdots\cdots \\
H^{(k)}_{0,j+1} - H^{(k)}_{1,j} - Z^{(k)}_{1,j}\left(Q^{(k)}_{0,j+1} - Q^{(k)}_{1,j}\right) - R^{(k)}_{1,j}\left|Q^{(k)}_{1,j}\right|^{m}\operatorname{sgn} Q^{(k)}_{1,j} = 0,
\end{gathered}
\tag{18}
$$

where: $H^{(1)}_{m1,j+1} = H^{(2)}_{0,j+1} = H^{(3)}_{0,j+1} = ... = H^{(k)}_{0,j+1} = H_{j+1}$

and the continuity equation:

$$
Q^{(1)}_{m1,j+1} = Q^{(2)}_{0,j+1} + Q^{(3)}_{0,j+1} + ... + Q^{(k)}_{0,j+1}, \tag{19}
$$

where superscripts (1), (2), ..., (k) denote the successive number of the pipeline.

Now let us take the following denotations:

$$
\begin{gathered}
S^{(1)} = -H^{(1)}_{m1-1,j} - Z^{(1)}_{m1,j}Q^{(1)}_{m1-1,j} + R^{(1)}_{m1,j}\left|Q^{(1)}_{m1-1,j}\right|^{m}\operatorname{sgn} Q^{(1)}_{m1-1,j} \\
S^{(2)} = -H^{(2)}_{1,j} + Z^{(2)}_{1,j}Q^{(2)}_{1,j} - R^{(2)}_{1,j}\left|Q^{(2)}_{1,j}\right|^{m}\operatorname{sgn} Q^{(2)}_{1,j} \\
\cdots\cdots\cdots\cdots\cdots\cdots\cdots\cdots\cdots\cdots\cdots\cdots\cdots\cdots\cdots\cdots\cdots\cdots\cdots\cdots\cdots\cdots \\
S^{(k)} = -H^{(k)}_{1,j} + Z^{(k)}_{1,j}Q^{(k)}_{1,j} - R^{(k)}_{1,j}\left|Q^{(k)}_{1,j}\right|^{m}\operatorname{sgn} Q^{(k)}_{1,j}.
\end{gathered}
\tag{20}
$$

Making use of the denotations and equations (18) and (19), the following equations were obtained:

$$
\begin{gathered}
H_{j+1} + Z^{(1)}_{m1,j}Q^{(1)}_{m1,j+1} + S^{(1)} = 0 \\
H_{j+1} - Z^{(2)}_{1,j}Q^{(2)}_{0,j+1} + S^{(2)} = 0 \\
\cdots\cdots\cdots\cdots\cdots\cdots\cdots \\
H_{j+1} - Z^{(k)}_{1,j}Q^{(k)}_{0,j+1} + S^{(k)} = 0.
\end{gathered}
\tag{21}
$$

Taking into consideration the compatibility equations (18) as well as the continuity equation (19), the following set of $(k+1)$ equations with $(k+1)$ unknown values is derived:

$$H_{j+1} = \frac{\dfrac{S^{(1)}}{Z^{(1)}_{m1,j}} + \dfrac{S^{(2)}}{Z^{(2)}_{1,j}} + \dfrac{S^{(3)}}{Z^{(3)}_{1,j}} + \cdots + \dfrac{S^{(k)}}{Z^{(k)}_{1,j}}}{\dfrac{1}{Z^{(1)}_{m1,j}} + \dfrac{1}{Z^{(2)}_{1,j}} + \dfrac{1}{Z^{(3)}_{1,j}} + \cdots + \dfrac{1}{Z^{(k)}_{1,j}}} \tag{22}$$

$$\begin{aligned} Q^{(1)}_{j+1} &= -\frac{H_{j+1} + S^{(1)}}{Z^{(1)}_{m1,j}} \\ Q^{(2)}_{j+1} &= \frac{H_{j+1} + S^{(2)}}{Z^{(2)}_{1,j}} \\ &\cdots\cdots\cdots\cdots\cdots\cdots \\ Q^{(k)}_{j+1} &= \frac{H_{j+1} + S^{(k)}}{Z^{(1)}_{1,j}}. \end{aligned} \tag{23}$$

Finally we receive the set of $(k+1)$ equations with $(k+1)$ unknown values. In the same way we can write appropriate equations for junctions with connecting pipelines and for complex junctions where several pipelines of positive and several pipelines of negative flow direction meet in the node.

5. Spatial Distribution of Pressure in Water Supply Looped Networks

Spatial distribution of pressure in water supply looped networks is illustrated by a case related to the analysis of a middle-sized water supply network in unsteady conditions. The network consists of 17 real loops, 48 pipelines and 33 nodes, supplied by two independent sources, i.e. from the upper water reservoirs (Fig. 15). When designing the water supply networks it is necessary to take into account the occurrence of some significantly high pressures that can be dangerous to the pipelines and appurtenances, e.g. hydrants, valves and fittings. The pressures are caused by instantaneous closure of the fluid flow at the end of any pipes, or due to failure of power to pump.

The calculations of water supply network in steady state conditions were carried out using of EPANET 2 software (Rossman 2000). In the calculations of the looped network in steady states advantage was taken of input data as presented by the scheme of pipe network in Fig. 15. The data include the number of the pipe, the length of the pipe section, and the nominal diameter, as well as information related to the nodes, as for instance, the node number, the external flow from the node, and the elevation of the node. It was assumed that the looped network would be made of cast iron flange pipes compatible with the appropriate Polish Standard.

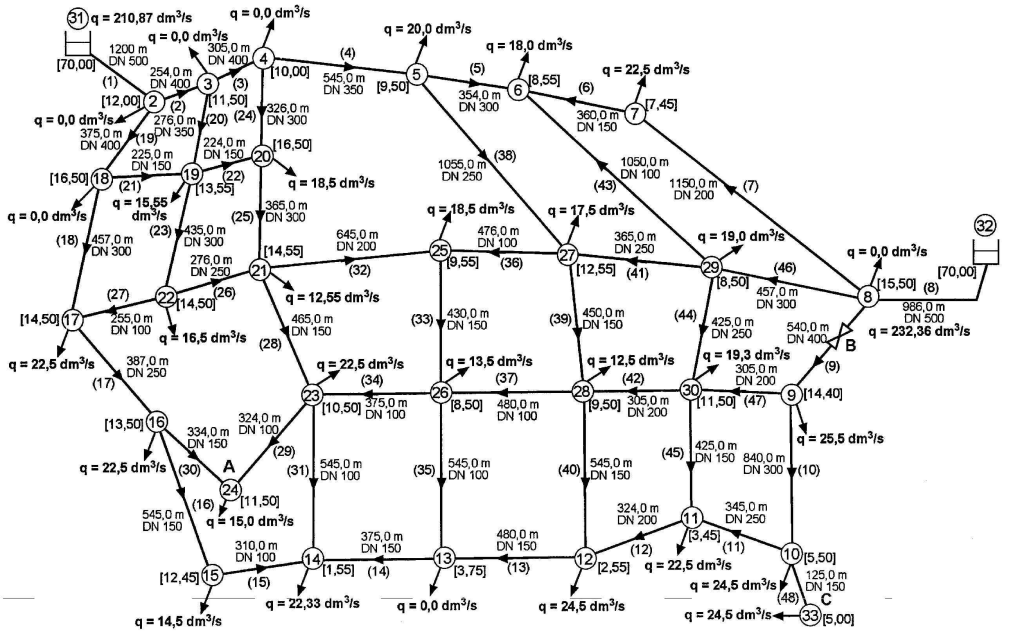

Fig. 15. Schematic diagram of water-pipe network for Example

The calculations of the looped pipe network in unsteady conditions were made using the computer programme based on the above presented method. The unsteady flows in the network of Fig. 15 were caused by closing of the ball valve in time $T_c = 5$ s, installed in the midpoint of pipe No. 9. The pipe of nominal diameter DN 400 and the total length $L = 540$ m is located in the vicinity of the upper reservoir supplying node No. 8 with water. The calculation results are presented in Figs. 16 to 18. The analysis of the obtained results indicates that the largest pressure increments occur in the middle of the pipe before the ball valve on the side of node No. 8 (Fig. 16). The maximum pressure head will reach 207.4 m of H_2O, while the minimum one will be 4.6 m of H_2O (Fig. 17). For this reason the higher pressure will be followed by pressure drop of 202.8 m, which is a magnitude twice as big as the permissible working pressure for cast iron flange pipes according to Polish Standard. The maximal value of the high pressure is in the permissible pressure range which in the case of cast iron flange pipes amounts to 2.5 MPa, that is about 250 m of H_2O. The increment of pressure to the maximal value will occur in this case in pipe 9 after the valve has been completely closed, i.e. after 5 s. Further pressure oscillations are characterized by an evident reduction of the extreme values and in fact after 30 s the pressure heads will be close to the steady state value being approximately 70 m of H_2O. The maximum pressure head at the end of pipe No. 8 connecting reservoir 32 with the network is 156 m of H_2O, and the minimum value of the reduced pressure is 18.7 m of H_2O.

However, the pressure oscillations around the steady state pressure amounting to approximately 60 m of H_2O undergo a relatively fast damping and after 12 s have no significance taking the pipeline strength into consideration. An examination of the extreme pressure heads in the remaining pipes outside pipe No. 9 where the flow disturbance occurred, has indicated that in this case we are dealing with remarkably large pressures in phases of higher values exceeding the permissible ones for cast iron pipes of ordinary wall thickness in 3 extra pipes, i.e. pipe No. 7 (node 7), pipe No. 46 (node 29), and in pipe No. 41 (node 27).

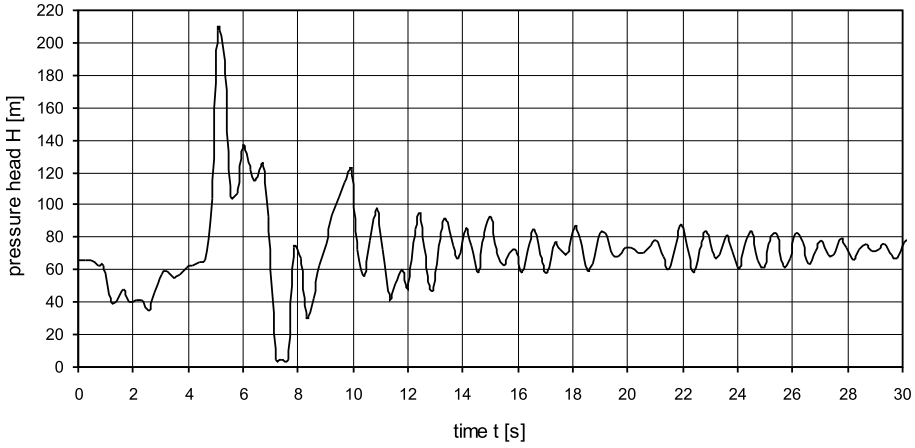

Fig. 16. Pressure head oscillations at midpoint of pipeline No. 9 (node No. 1)

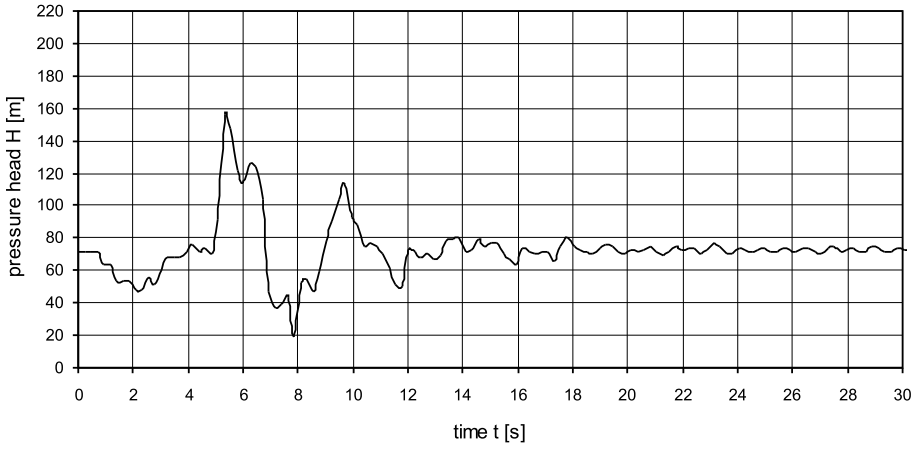

Fig. 17. Pressure head oscillations at the final cross-section of pipeline No. 8 (node No. 8)

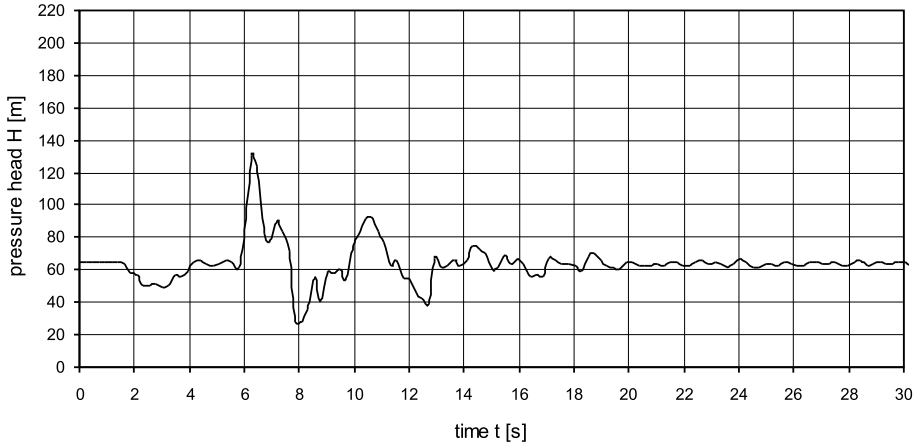

Fig. 18. Pressure head oscillations at the final cross-section of pipeline No. 7 (node No. 7)

As can be seen in Fig. 16 pipe No. 7 and 46 have a direct connection with node 8, and pipe 41 is situated further off pipe No. 29, but the flow intensity in this pipe is significantly great reaching 37.69 dm^3/s. The maximum and minimum pressure heads at some selected nodes are as follows:

- H_{max} = 130.6 m, H_{min} = 28.0 m of H_2O at the end of pipe No. 7 (node 7),
- H_{max} = 114.1 m, H_{min} = 22.4 m of H_2O at the end of pipe No. 46 (node 29),
- H_{max} = 90.80 m, H_{min} = 18.5 m of H_2O at the end of pipe No. 47 (node 30),
- H_{max} = 89.30 m, H_{min} = 41.9 m of H_2O at the end of pipe No. 43 (node 6),
- H_{max} = 104.1 m, H_{min} = 20.7 m of H_2O at the end of pipe No. 41 (node 27),
- H_{max} = 88.50 m, H_{min} = 42.8 m of H_2O at the end of pipe No. 38 (node 5),
- H_{max} = 54.10 m, H_{min} = 30.8 m of H_2O at the end of pipe No. 14 (node 14),
- H_{max} = 83.30 m, H_{min} = 50.2 m of H_2O at the end of pipe No. 26 (node 22).

This illustrative example proves that the extreme pressure heads in unsteady state in pipes situated much further away from the disturbance source, and particularly in the case of pipe No. 14, are insignificant since the pressure head increment in the phase of higher pressure attains 21.1 m of H_2O, and the maximum pressure head reduction reaches only 2.2 m of H_2O with regard to stationary conditions. The analysis of an arbitrary water supply looped network should therefore refer to pipes situated as close to the source of flow disturbance as possible.

6. Summary and Final Conclusions

1. The main purpose of the paper was to present an adequate method for the analysis of transient flows in water pipe networks. The partial differential

equations of hyperbolic type, describing the phenomenon, have been transformed by the method of characteristics (MOC) into ordinary differential equations, i.e. compatibility equations on appropriate characteristics. In the paper the concept of fix grid of characteristics for MOC is presented.

2. In the numerical calculations advantage has been taken of the iterative procedure referred to as the predictor-corrector method which can be used in the cases when frictional effects are very important. In this method the corrected values of the pressure heads $H(x,t)$ and discharge flows $Q(x,t)$ are calculated on the basis of the mean resistance of elementary pipe sections related to the flow value of the preceding and following time steps.
3. The correctness of the applied method of characteristics for analysis of transient flow with regard to single straight pipes has been verified by the use of our own unsteady flow experiments performed on an experimental installation situated in the Hydraulic Laboratory at the Faculty of Environmental Engineering, Warsaw University of Technology. Advantage was also taken of the investigation results made available by Pezzinga from the Institute of Hydraulics, Hydrology and Water Management, University of Catania (Italy).
4. The calculation results are in both cases in good conformity with experimental data. The comparisons show that the average error of maximum oscillations is 1.2% to 2.4%, the average error of minimum oscillations is 10% to 15% in the case of our own measurements, the average error of maximum oscillations is 1% to 3% and the average error of minimum oscillations is 10% to 12% in the case of measurements by Pezzinga.
5. The proposed verified method of hydraulic transients analysis in the case of simple pipes could also have a practical meaning in the case of pipe networks analysis, as the phenomenon in complex pipeline system is similar. The main difference lies in some additional boundary conditions in pipe networks.
6. In the numerical calculations of the pipe networks in unsteady state, attention was mainly concentrated on spatial analysis of pressure distribution caused by local variation of flow conditions. It has been proved that in all the cases under consideration the obtained pressure head increments for a pipe or pipes where the discharge flow was being closed were very high. In all other pipes the maximum pressure heads are lower than their adequate permissible pressure values and/or test pressure for the pipe material.
7. The lack of appropriate domestic and foreign publications dealing with the achievements in the field of transient flows in pipe network causes difficulties in verifying the proposed calculation method. Therefore the numerical calculation results presented in the paper, that have been verified on the basis of measurements performed for a single pipe, should be treated as partly

verified model of such complex phenomenon as the transient flow of liquid in closed pipelines.

8. According to the latest researches it follows that the reason for faster attenuation of pressure head oscillation should be looked for among the so-called relaxation processes which include a group of phenomena causing irreversible conversion of potential mechanical energy into heat, in particular occurring in the pipe's wall. An analysis of the physical aspects of the phenomenon leads to the conclusion that besides the viscous mechanism of the energy losses it is necessary to take into account the relaxation factors. As a result of such an approach to the problem, efforts have been made to introduce relaxation friction factor λ_r to the friction element, which can easily be considered in traditional software as corrected friction factor.
9. The problem of linear friction resistance in transient flow is still open and inspires many researches. However, it is not the object of this paper. Our own experimental tests have proved that the values of the relaxation factor of friction losses λ_r are bigger in the range of 5 to 10 times than the calculated values of the factor obtained from the Colebrook-White equation. The experimental tests have indicated that a greater compatibility between the calculations and measurements takes place for cross-sections at the valve mounted at the end of the pipeline. However, larger discrepancy has been noted in the case of mid-length of pipe, or any cross-section around the pipe except the final section close to the valve.

References

Axworthy D. H., Ghidaoui M. S., McInnis D. A. (2000), Extended thermodynamics derivation of energy dissipation in unsteady pipe flow, *Journal of Hydraulic Engineering, Proceedings of ASCE*, Vol. 126, No. 4, 276–287.

Bergant A., Simpson A. R. (1994), Estimating unsteady friction in transient cavitating pipe flow, *The 2nd International Conference on Water Pipeline Systems*, Proceedings, Edinburgh, Scotland, 3–15.

Bergant A., Simpson A. R., Vitkovsky J. (1999), Review of unsteady friction models in transient pipe flow, *9th International Meeting on the Behaviour of Hydraulic Machinery Under Steady Oscillatory Conditions*, International Association of Hydraulic Research, Brno, Czech Republic, Paper D1, 1–11.

Brunone B., Golia U. M., Greco M. (1991), Some remarks on the momentum equations for fast transients, *International Meeting on Hydraulic Transients with column separation, 9th Round Table, IAHR*, Valencia, Spain, 201–209.

Chaudhry M. H. (1979), *Applied Hydraulic Transients,* Van Nostrand Reinhold Company, New York.

Evangelisti G. (1969), Waterhammer analysis by the method of characteristics, *L'Energia Elettrica*, Nos. 10–12.

Fox J. A. (1977), *Hydraulic Analysis of Unsteady Flow in Pipe Networks*, The Macmillan Press Ltd, London and Basingstoke.

Jeppson R. W. (1976), *Analysis of Flow in Pipe Networks*, Ann Arbor Science Publishers, Inc., Ann Arbor, Michigan.

Karney B. W., McInnis D. (1992), Efficient calculation of transient flow in simple pipe networks, *Journal of Hydraulic Engineering*, Vol. 118, No. 7, 1014–1030.

McInnis D., Karney B. W. (1995), Transients in distribution networks: field tests and demand models, *Journal of Hydraulic Engineering, Proceedings of ASCE*, Vol. 121, No. 3, 218–231.

Pezzinga G., Scandura P. (1995), Unsteady flow installations with polymeric additional pipe, *Journal of Hydraulic Engineering, Proceedings of ASCE*, Vol. 121, No. 11, 802–811.

Pezzinga G. (1999), Quasi-2D model for unsteady flow in pipe networks, *Journal of Hydraulic Engineering, Proceedings of ASCE*, Vol. 125, No. 7, 676–685.

Pezzinga G. (2000), Evaluation of unsteady flow resistance by quasi-2D or 1D models, *Journal of Hydraulic Engineering, Proceedings of ASCE*, Vol. 126, No. 10, 778–785.

Rossman L. A. (2000), *EPANET 2. Users Manual,* Water Supply and Water Resources Division, National Risk Management Research Laboratory, Office of Research and Development, U.S. Environmental Protection Agency, Cincinnati, Ohio.

Samani H. M. V., Khayatzadeh A. (2002), Transient flow in pipe networks, *Journal of Hydraulic Research*, Vol. 40, No. 5, 637–644.

Streeter V. L. (1967), Water-hammer analysis of distribution systems, *Journal of the Hydraulics Division, Proceedings of the ASCE*, Vol. 93, No. HY5, 185–201.

Streeter V. L. (1972), Unsteady flow calculations by numerical methods, *Proceedings of the ASME, Journal of Basic Engineering*, Vol. 94, series D, No. 2, 457–466.

Vitkovsky J., Lambert M., Simpson A., Bergant A. (2000), Advances in unsteady friction modeling in transient pipe flow, *The 8th International Conference on Pressure Surges, BHR*, The Hague, The Netherlands, 587–597.

Wichowski R. (1999), Unsteady Flow Analysis in Water Supply Networks – Part I, *Archives of Hydro-Engineering and Environmental Mechanics*, Vol. 44, No. 1–4, 3–29, Part II, *Archives of Hydro-Engineering and Environmental Mechanics*, Vol. 44, No. 1-4, 31–62.

Wichowski R. (2002), *Selected Problems of Unsteady Flows in Pipe Networks of Water Supply Systems*, Politechnika Gdańska, Monografie 27, (in Polish).

Wood D. J., Lingireddy S., Boulos P. F., Karney B. W., Mcpherson D. L. (2005), Numerical methods for modeling transient flow in distribution systems, *Journal AWWA*, Vol. 97, No. 7, 104–115.

Wylie E. B., Streeter V. L., Suo L. (1993), *Fluid Transients in Systems,* Prentice Hall, Inc. A Simon & Schuster Company, New Jersey Englewood Cliffs, NJ 07632.